



Cite this: *Phys. Chem. Chem. Phys.*,
2024, 26, 15205

Code generation in ORCA: progress, efficiency and tight integration†

Marvin H. Lechner, *‡ Anastasios Papadopoulos, *‡ Kantharuban Sivalingam, Alexander A. Auer, Axel Koslowski, Ute Becker, Frank Wennmohs and Frank Neese *

An improved version of ORCA's automated generator environment (ORCA-AGE II) is presented. The algorithmic improvements and the move to C++ as the programming language lead to a performance gain of up to two orders of magnitude compared to the previously developed `PYTHON` toolchain. Additionally, the restructured modular design allows for far more complex code engines to be implemented readily. Importantly, we have realised an extremely tight integration with the ORCA host program. This allows for a workflow in which only the wavefunction Ansatz is part of the source code repository while all actual high-level code is generated automatically, inserted at the appropriate place in the host program before it is compiled and linked together with the hand written code parts. This construction ensures longevity and uniform code quality. Furthermore the new developments allow ORCA-AGE II to generate parallelised production-level code for highly complex theories, such as fully internally contracted multireference coupled-cluster theory (fic-MRCC) with an enormous number of contributing tensor contractions. We also discuss the automated implementation of nuclear gradients for arbitrary theories. All these improvements enable the implementation of theories that are too complex for the human mind and also reduce development times by orders of magnitude. We hope that this work enables researchers to concentrate on the intellectual content of the theories they develop rather than be concerned with technical details of the implementation.

Received 30th January 2024,
Accepted 6th May 2024

DOI: 10.1039/d4cp00444b

rsc.li/pccp

Introduction

The boundaries of what is possible in quantum chemistry are continually being expanded, not least through advancements in microprocessor technology. Over the last decades, feasible *ab initio* wave function-based calculations have progressed from simple, SCF-level calculations in small basis sets^{1,2} to production level application of advanced correlated methods. For instance, the coupled cluster (CC) model can now be applied to medium to large molecules in triple- ζ or even larger basis sets,³ or even very large molecules when local approximation techniques are employed.^{4,5} This development has been fostered in great part by the advances in CPU processing power, commonly described by Moore's law.⁶ It is the opinion of the authors that these advances bring more and more computationally demanding theories into the realm of "routinely feasible" computations. These theories include internally

contracted^{7,8} (ic) multireference (MR) theories and gradients of higher-order CC models, the implementation of which is, in fact, beyond human capacity. Traditionally, a quantum chemical theory would be reformulated for and implemented in computer code entirely manually, which is an onerous and error-prone⁹ approach. In light of these challenges, tools have been developed that either simplify or completely automate the implementation process, which we will refer to as automatic code generation. These tools automate at least one of the following general steps needed to go from theory on paper to computer code: (i) derivation of the working equations from an Ansatz (equation generation), (ii) manipulation thereof to reduce the computational cost (factorization), and (iii) the actual code generation. We will adopt this distinction throughout the rest of this paper and expand on each of the steps below. For a more detailed introduction to the field of automatic code generation, we also recommend the excellent review of Hirata.¹⁰

Automatic derivation of the working equations from a theoretical Ansatz is the most straightforward part, since it mostly relies on a fixed set of rules that can be applied deterministically. Very early on in the development of equation generation¹¹ Wick's theorem^{12,13} was used in order to obtain the explicit

Department of Molecular Theory and Spectroscopy, Max-Planck-Institut für Kohlenforschung, Kaiser-Wilhelm-Platz 1, 45470 Mülheim an der Ruhr, Germany.
E-mail: frank.neese@kofo.mpg.de

† Electronic supplementary information (ESI) available. See DOI: <https://doi.org/10.1039/d4cp00444b>

‡ These authors share first authorship.



forms of the tensor contractions. Even today most existing toolchains^{14–28} rely on the same principle. Despite this prevalence of Wick's theorem, the first automated equation generators used diagrammatic approaches, mainly to avoid tedious and error prone derivations by hand.^{29–31} However, these early developments lack further equation processing and code generation. A major benefit of diagrammatic generators is that only topologically different contractions are generated, *i.e.*, less work needs to be done in finding equivalent terms in the factorization step.¹⁶ More recent examples of such equation generators are Smith¹⁶ by Shiozaki and co-workers or the arbitrary-order CC program by Kállay and Surján (MRCC).³² In our own work, we have used neither approach, but instead relied on plain and simple (anti-)commutation rules between second-quantized operators that are applied recursively until all non-target labels have been processed.³³ This strategy was adopted in the first version of the ORCA-AGE toolchain and has the advantage that it can be applied equally well to single- or multireference reference functions.³⁴

The factorization step is arguably the most crucial in the toolchains, since it ensures the proper, minimal computational scaling with system size and significantly reduces the computational cost of the generated code. Unfortunately, finding the global minimum in terms of computational cost constitutes an NP-hard problem.³⁵ Hence, virtually all toolchains rely on heuristics to reduce the complexity of this problem. Core concepts were developed early on, *e.g.*, by Janssen and Schaefer¹¹ or Kállay and Surján.³² However, perhaps the most complete overview can be found in the literature describing the tensor contraction engine (TCE),^{14,15} which sequentially uses detection of duplicates, strength reduction, factorization (*i.e.*, application of the distributive law), and common subexpression elimination to arrive at the final working equations before generating code.¹⁴ Tensor contractions are often canonicalized by relabelling and permuting the indices and tensors in order to aid in detecting duplicate terms, cancelling terms and common subexpressions, especially when taking tensor symmetry into account.^{11,14,35–37} A detailed analysis of common subexpression elimination was published by Hartono *et al.*³⁸ Overall, these heuristics perform quite well,³⁹ although they will generally not reach the same efficiency as the best hand-optimized⁴⁰ code. More advanced schemes have been discussed,³⁵ but, to the best of our knowledge, only a single tool that uses a genetic algorithm to sample the complete factorization space has been presented to date.³⁹ An overview of the algorithms used in the AGE can be found in the original publication.³⁴

Finally, the equations that have been derived, canonicalized and factorized in the previous steps must be evaluated (in the correct order) in order to arrive at the desired implementation of the target quantity, which may, for example, be an energy or a residual. To this end, we can either generate code (generally for a compiled programming language) or use an interpreter to evaluate the tensor contractions. Generated code frequently relies on further libraries, most often on the basic linear algebra subroutines (BLAS)⁴¹ to speed up the evaluation

of the tensor contractions. BLAS can be extended to arbitrary (binary) tensor contractions,⁴² and even faster algorithms have been developed for the same sake.⁴³ As an intermediate between low-level generated code and interpreters, specialized tensor contraction libraries have emerged that more or less completely take care of the computational kernel such that code generation can be greatly simplified. Examples of such libraries include the CTF,^{44,45} libtensor,⁴⁶ LITF,⁴⁷ TCL,^{43,48} and TiledArray.^{49,50} Interpreters even further remove the connection of the contractions to the (compiled) code or hardware by fully abstracting away the latter two, requiring just the contractions and the input quantities. This concept is perhaps best illustrated with the super instruction assembly language (SIAL) of ACES III, which is a full-fledged virtual machine and parallel programming model⁵¹ used to evaluate generated and handwritten contractions.^{52,53} An integrated tensor framework (ITF) has been reported by Werner and co-workers for the implementation of an internally contracted multireference configuration interaction (ic-MRCI) method.^{18,54} Other toolchains with interpreters using string-based methods^{31,55} include the general contraction engine (GeCCo) by Köhn and co-workers, first to appear in the context of explicitly correlated coupled cluster methods,^{27,28} and Kállay and Surján's arbitrary-order CC program.^{32,56}

To conclude the introduction, we now briefly discuss applications of existing code generators. One of the most complete implementations remains the TCE,^{14,15} which encompasses all the steps outlined above. Generated code exists in NWChem,^{57,58} and examples include higher-order CC methods (up to (EOM)-CCSDTQ)⁵⁹ or combined CC theory and MBPT.⁶⁰ The SMTH generator by Shiozaki and co-workers,^{16,17} which can be viewed as the successor to the TCE,⁶¹ is another feature-complete tool that was initially used to implement CCSD-R12,⁶¹ and later extended to state-specific¹⁷ and multistate⁶² CASPT2 gradients. Around the same time, the SQA, used for the automatic implementation of CT theory^{19,20} and later for the MR-ADC(2) method,^{63,64} and FEMTO codes^{21–23} were introduced. FEMTO has specialized features to work with cumulant reconstructions that appear in internally contracted DMRG-MRCI theory, and has also been extended to pair-natural orbitals (PNOs).²³ Also noteworthy are the GeCCo^{27,28} and APG^{24–26} codes, which have both been used to implement highly complex ic-MR methods, such as fully internally contracted multireference coupled cluster theory (fic-MRCC)⁶⁵ and MR-EOMCC^{66–69} theory, respectively. More recently, GeCCo and ITF have been used together to develop an optimised fic-MRCC implementation.⁷⁰ For a long time, the APG and SQA were the only tools that supported Kutzelnigg–Mukherjee normal order,⁷¹ with generalized normal order (GNO) being taken up more recently by the Wick&d program⁷² of Evangelista. Last but not least, the first version of the ORCA-AGE toolchain was introduced close to seven years ago.³⁴ Different multireference contraction schemes were compared with its support,⁷³ and the STEOM method based on an unrestricted Hartree–Fock (UHF) reference has been implemented⁷⁴ with the aid of the APG into the ORCA^{75–77} program package.



In this article, we describe a completely rewritten and vastly improved ORCA-AGE toolchain, henceforth referred to as ORCA-AGE II. Thus, we first outline the differences to the previous version of the toolchain and the numerous improvements that have been incorporated. Furthermore, we will compare its features to other existing solutions. Then, we showcase recent developments, most of which have only been possible through the improvements made to the toolchain. We will finish with a holistic view of and perspective for the development process in quantum chemistry, including our vision for the ORCA^{75–77} program package. Lastly, we conclude by summarizing the main points of this article.

Software description

The ORCA-AGE II toolchain has been rewritten from scratch, a decision that has been motivated by the experience gained while working with its first version.³⁴ In this section, we first recapitulate the layout of ORCA-AGE II, which has mainly undergone streamlining, before we discuss the new internal algorithms, equation and code generators. Further information on the code generation process can be found in the preceding publication.³⁴

From an architectural standpoint, ORCA-AGE II still uses the modular structure of its predecessor, organized into three groups: equation generation, equation processing (factorization), and code generation. Each of these three steps is further split into smaller executables that only perform a very specific subtask, *e.g.*, merging several contractions into one by exploiting tensor symmetry. This layout allows highly flexible workflows, where each step can be turned on or off depending on the user's preference, although all steps are enabled by default to achieve the best possible performance of the generated code. In turn, each of these steps may have optional features like debug output or different contraction engines, which are controlled through easy-to-understand command line options as well. Furthermore, the user can easily verify or modify all intermediate stages, which are simply text files containing a single contraction per line, as necessary. An example of such an equation file is given in Scheme 1.

Here, the indices indicate the orbital space they belong to, using i, j, k, l for inactive, t, u, v, w for active, and a, b, c, d for virtual orbitals. Furthermore, any index has a number asso-

ciated with it, so that a unique index can always be constructed. Finally, a capitalised label indicates a summation index.

While the general structure of the toolchain has remained largely unchanged, the code itself is an entirely new development. The main reason for redeveloping the software lies in the long code generation times of the previous version, which required about one month to generate highly complicated theories such as fic-MRCC, leading to a slow overall development and debugging process. This was addressed by improving the internal algorithms throughout all factorization and generation steps. For example, we introduced a hash-based data compaction method for eliminating duplicate intermediates generated by the initial, term-wise factorization step. This reduces the scaling from a quadratic to an expected linear-time algorithm, and consequently to a speedup of about two orders of magnitude for the fic-MRCC method in this step alone. While this example shows the biggest improvement over the old toolchain, other parts, such as the detection of tensor symmetry, have received improvements of up to one order of magnitude as well. To further ensure good use of multicore architectures, we use OpenMP to allow for thread-based parallelism in the toolchain. Lastly, the new toolchain has been written in the C++ programming language, which together with an improved factorization algorithm, is responsible for a large part of the speedups compared to the previous implementation that relied on PYTHON. Another benefit of relying on C++ is that ORCA-AGE II fits far better into the ORCA ecosystem through a more homogeneous and cleaner software structure. Taken together, the parallelized and improved C++ code allows us to generate and process highly complex equations in minutes rather than weeks that were required for the serial PYTHON code.

Internally, the executables rely on a core library that provides the required basic functionality to read/write, represent, and manipulate tensor contractions as a set of high-level classes and functions. This library, and by extension the entire toolchain, has no limitations in terms of number of indices per tensor, allowed tensor symmetries, or number of source tensors per contraction, to name a few features. Consequently, any theory that can be written as a set of tensor contractions can be implemented with ORCA-AGE II. Also, despite this generality, even costly operations such as determining the tensor symmetry of an intermediate based on its source tensors are so fast that they can be routinely used for hundreds of tensors with, for example, ten indices, as is the case in fic-MRCC theory (further discussed below).

In addition to the improvements to the underlying infrastructure, the functionality (especially of the code generator) has been extended as well. In terms of performance improvements, the recent work falls into the two categories of compute and I/O optimizations. We first discuss the compute optimizations, which are mainly geared towards making BLAS calls more pervasive in the generated code. To this end, we use the fact that essentially every binary tensor contraction can be written as a matrix–matrix multiplication,

$$C_{ij} = \sum_k A_{ik} B_{kj}, \quad (1)$$

```

Sijab(a0,i0,b0,j0) += -1 FC(j0,I1) Cijab(b0,I1,a0,i0)
Sijab(a0,i0,b0,j0) += -1 FC(i0,I1) Cijab(a0,I1,b0,j0)
Sijab(a0,i0,b0,j0) += 1 FC(b0,A1) Cijab(A1,j0,a0,i0)
Sijab(a0,i0,b0,j0) += 1 FC(a0,A1) Cijab(A1,i0,b0,j0)
Sijab(a0,i0,b0,j0) += 1 I(I1,j0,I2,i0) Cijab(b0,I1,a0,I2)
Sijab(a0,i0,b0,j0) += -1 I(I1,j0,b0,A1) Cijab(A1,I1,a0,i0)
Sijab(a0,i0,b0,j0) += -1 I(I1,i0,a0,A1) Cijab(A1,I1,b0,j0)
Sijab(a0,i0,b0,j0) += -1 I(I1,j0,a0,A1) Cijab(b0,I1,A1,i0)
[...]
CorrelationEnergy() += -1 I(I0,A1,I1,A0) Cijab(A0,I0,A1,I1)
CorrelationEnergy() += 2 I(I0,A0,I1,A1) Cijab(A0,I0,A1,I1)
[...]

```

Scheme 1 Equation file for RHF CID Sigma equations.



in which the “compound” indices i, j, k may refer to none, one, or multiple actual indices. As a result, outer products and matrix–vector and vector–vector multiplications can be viewed as special cases thereof. Such a scheme has already been discussed in the literature, and is generally referred to as “transpose–transpose–DGEMM–transpose” (TTGT), since (in the worst case) we might need to reorder (transpose) the axes (indices) on both source tensors and the target tensor.^{42,43} To the best of our knowledge, none of the previous implementations are as general as the current implementation in ORCA-AGE II, as our implementation also allows for further edge cases (trace operations, repeated indices, ...) as well as an I/O-aware strategy for indices associated with an I/O read/write penalty. Moreover, indices can be individually pulled out from the tensor contraction to be processed in outer for-loops, which is highly useful for integrating the TTGT engine with other specialized functions as well as enabling relatively straightforward parallelization over these outer loops. Effectively, such situations are handled automatically by reordering and “tiling”¹⁴ the tensors such that the chunks can be treated most efficiently with DGEMM operations that are as large as the available memory allows working on tensors that are trivial to fetch from disk or memory. This scheme is especially useful for compute-bound scenarios,⁴³ e.g., contractions involving large and high-dimensional objects such as the four- and five-body densities, γ_4 and γ_5 , respectively. Naïve loop-based code, by construction, will lead to many cache misses and is generally up to a factor of 100 slower than the optimized, BLAS-based contraction scheme, especially tensors that require many MBs or even GBs of storage.

Also in the category of compute optimizations are further hand-coded routines. Additional contraction patterns have been added to the “ContractionEngine” functionality for increased performance, which complement the features already available since the first version of the code generator.³⁴ These patterns are especially useful for the generation of analytic gradients components (*vide infra*).

On the note of I/O improvements, we should first delineate how ORCA-AGE II deals with a mixed strategy of keeping some tensors on disk and some entirely in memory. Ultimately, the decision is up to the end user, but by default 4-index quantities are stored on disk with two indices encoding disk access, for which a matrix can be retrieved. In the ORCA framework these objects are called “matrix containers” and they have been part of the ORCA infrastructure since the earliest days of the correlation modules. The matrix containers are intrinsically “smart”, in that they automatically take care of storage of the data in memory or on disk in an uncompressed or compressed format and they also distribute data across the available disks with the programmer that uses these objects having to write a single line of additional code. The tools can deal with symmetric or unsymmetric matrices, vectors and, ultimately, with arbitrary dimensional tensors *via* another tool, we have called “MultiIndex” that allows us to generate arbitrarily complex compound indices from any set of individual indices. For example, given X_{pq}^{rs} and using the lower indices for access, we

can load matrices of $r \times s$ for a given index pair p, q . In ORCA-AGE II, these quantities are generally stored on disk to integrate nicely with the rest of the ORCA infrastructure as well as to avoid memory bottlenecks (e.g., the 4-external integrals ($ab|cd$) already exceed 10 GB for $n_{\text{virt}} > 188$ virtual orbitals in double precision).

We optimized the I/O performance by both hand-coded contractions and a new on-the-fly resorting scheme. The hand-coded functions are mostly geared towards copy/add operations,

$$C_{ij\dots} \leftarrow A_{\Pi(ij\dots)}, \quad (2)$$

which repeatedly occur through the application of the distributive law. Here, $\Pi(ij\dots)$ denotes an arbitrary permutation of indices on the source tensor. These functions are tailored to the 4-index tensors that are stored on disk. Throughout the generated code, we try to minimize contractions that have different addressing indices by determining the best index order on the intermediates, but I/O-intensive contractions such as

$$X_{pq}^{rs} \leftarrow Y_{rs}^{pq}, \quad (3)$$

where none of the addressing (lower) indices match, cannot always be avoided. Addressing indices refer to indices that are used to retrieve a matrix from a data container. For instance, tensor X_{pq}^{rs} in eqn (3) would have addressing indices p, q that are used to retrieve a matrix (typically from disk) with dimensions r, s . In a naïve implementation, this will lead to I/O operations being done in inner loops, with the associated increase in runtime due to disk latency and unnecessary repetitions of I/O operations. To alleviate the I/O bottleneck of these additions, special functions were coded that read batches of the tensors up to the allowed memory limit, do the operation in memory, and then efficiently write the results back to disk.

A more general scheme was also introduced that proceeds by resorting the on-disk quantities on the fly. The underlying inefficiency is the same as discussed above, namely, that non-matching indices are associated with I/O operations. In the general case, however, we do not opt for a batching scheme, but rather exploit the fact that reordering such a 4-index tensor only scales as $\mathcal{O}(N^4)$ and can be done itself with efficient hand-written functions. Virtually all contractions that use such stored quantities scale higher than $\mathcal{O}(N^4)$, and hence the additional reordering step is negligible in cost. Furthermore, these resorted matrix containers can be kept until the end of the computation to be reused in multiple contractions, at the expense of additional disk space being used. Nonetheless, since disk space is generally not limiting for highly correlated theories, we found this strategy to improve computational efficiency by at least a factor of 10 for larger examples while increasing disk space by only a marginal amount.

Compared to the first ORCA-AGE toolchain, the updated version has also been integrated much more tightly with the main ORCA source code. The philosophy of this approach will be discussed in detail at the end of this paper.

Comparison to other toolchains

To summarize the features of ORCA-AGE II and show how it relates to other code generators used in quantum chemistry, we summarized the main code generation features in Table 1. To keep the size of the table manageable, we only included other codes that are sufficiently complete or have been more widely used.

We now highlight a few salient features of the tools from Table 1. First, only ORCA-AGE relies on a commutator-based engine to derive the working equations for simplicity and generality. However, using a Wick's theorem or diagram-based engine can be significantly faster and reduce the time required to remove equivalent contractions. Hence, efforts to develop such an engine are ongoing for ORCA-AGE II. Second, great care is placed by all toolchains on a complete factorization toolchain, which is a testament to the importance of this step in obtaining a performant implementation. Third, the actual evaluation part either relies on generation of actual code or simply interprets the factorized equations akin to a specialized virtual machine. To this end, all toolchains except for one rely on BLAS to maximize computational efficiency. Parallelization support, however, is not implemented for all toolchains since doing so in a completely automated fashion is highly non-trivial.

Recently implemented methods with ORCA-AGE II

With the new, improved ORCA-AGE II toolchain, we now find ourselves in a position where large, complicated theories can be implemented quickly into the ORCA software package. In this section, we will demonstrate a few examples, starting with the CCSDT method and its various approximations. Then, going on to theories that contain more tensor contractions, we show how ORCA-AGE II can also generate gradients for CI and CC theories with minimal effort. We then conclude this section with details of our fci-MRCC implementation, which contains so many terms that it is beyond human capacity to implement.

CCSDT

As more powerful hardware and successively more efficient implementations of post-HF methods started being available, methods like CCSD(T) established themselves as what today is called “gold standard” in quantum chemistry.⁷⁹ One aspect that can be considered as crucial in this respect is the availability of excitations higher than doubles, and hence, especially during the 1980s many pioneering efforts were made towards efficient and powerful implementations of variants of CCSDT methods and beyond, like CCSDT(Q).⁸⁰ In line with some of the existing multireference approaches, CCSDT and CCSDTQ energies and their analytical derivatives are among the most complex and challenging algorithms that have been implemented and optimized by hand.^{81,82}

Table 1 Overview and comparison of several code generators used in quantum chemistry with ORCA-AGE II. An ‘x’ indicates that the feature of that column is supported by the software, a ‘—’ signifies the absence, and ‘n/a’ stands for ‘not applicable.’ For the equation generation columns, we indicate whether commutator algebra, Wick’s theorem with normal order, or diagrams are used to derive the working equations. In the factorization step, the codes may support detection of duplicates, strength reduction for tensor contractions, using the distributive law (sometimes called ‘factorization’) to reduce the prefactor, and (sub)expression elimination. For code generation, we indicate whether the generator directly produces ‘plain’ code, i.e., code not relying on external libraries, or whether it uses external libraries or interprets the equations directly. We further indicate if a string-based approach is used, and whether the BLAS library is employed. Lastly, we specify whether parallelized code can be produced. The main references for the programs are: FEMTO,^{21–23} SQA,¹⁹ Smith3,^{17,78} Smith,^{16,61} TCE,¹⁵ GeCCo,^{27,28} ORCA-AGE,³⁴ ORCA-AGE II (this work), MRCC⁵⁶

Program	Equation generation			Factorisation			Code generation			Parallel	BLAS	String	Interpreter	(Sub)expression elimination	“Plain” code	Partial	Strength reduction	Duplicates	Diagrams	Commutation	Wick/NO
	Equation generation	Factorisation	Code generation	Equation generation	Factorisation	Code generation	Equation generation	Factorisation	Code generation												
FEMTO	—	x	—	x	x	x	—	—	x	—	—	x	x	x	x	x	x	x	x	x	2013
SQA	—	x	—	x	x	x	—	—	x	—	—	x	x	x	x	x	x	x	x	x	2009
Smith3	—	x	Internal ^a	n/a	x	x	x	—	x	—	—	x	x	x	x	x	x	x	x	x	2015
Smith	—	—	n/a	n/a	x	x	x	x	x	—	—	x	x	x	x	x	x	x	x	x	n/a
TCE	—	x	—	x	x	x	x	x	x	—	—	x	x	x	x	x	x	x	x	x	2008
GeCCo	—	x	Internal ^a	x	x	x	x	x	x	—	—	x	x	x	x	x	x	x	x	x	2008
ORCA-AGE	x	—	In progress	—	x	x	x	x	x	x	—	x	x	x	x	x	x	x	x	x	2017, 2024
MRCC	—	—	x	n/a	x	x	x	x	x	—	—	x	x	x	x	x	x	x	x	x	2001

^a While generating terms with Wick’s theorem, topologically equivalent terms (diagrams) can be recognized and combined.



Hence, it is not surprising, that many of the early computer-aided implementation techniques in quantum chemistry focused on generating higher order coupled cluster methods or MR-CC implementations. The CCSDT method can be viewed as a standard example for high complexity of equations with numerous terms, complex tensor contractions and high-dimensional wavefunction parameters. For this reason, we will discuss the ORCA AGE implementation of the UHF CCSDT-1 and CCSDT energies in detail in the following. This does not only present an illustrative example but also demonstrates the versatility and simplicity of the tools available and allows for a conceptual comparison with other code generation tools.

Besides perturbative triples corrections, iterative CCSDT approximations like the CCSDT- N ($N = 1, 2, 3$ and 4) have been proposed as a systematic hierarchy of approximations with reduced computational effort.^{83–89} While CCSDT-1, 2 and 3 exhibit $\mathcal{O}(N^7)$ scaling, CCSDT-4 includes $T_3 \rightarrow T_3$ terms which scale as $\mathcal{O}(N^8)$ and only two contributions to the triples equations are excluded from the full CCSDT amplitude equations. In order to generate all of these approximations, it is essential that the generation tool allows to evaluate the nested commutator expressions from the Baker–Campbell–Hausdorff (BCH) expansion as well as the addition of separate commutator terms to an existing set of equations. ORCA-AGE II can do both as we will show in the following.

Before going into the full input listing for the CCSDT- N theories, we will start with UHF-CCSD to show a simplified connection to the conventional equations (Scheme 2). This is accomplished by simply specifying the maximum level of nested commutators that should appear in the energy and residual equations in \$order_E and \$order_residuals, respectively. Lastly, each \$class line provides an identifier, an amplitude, the excitation operators contained in the cluster operator \hat{T} , and (optionally) contravariant projection functions⁹⁰ for the residuals after a semi-colon. The E -operators contained therein typically refer to spin-traced operators \hat{E}_q^p , but in the case of UHF references they refer to pairs of elementary creation and annihilation operators in spin-orbital basis, $\hat{a}^{p\sigma}\hat{a}_{q\sigma}$. The rest of the infrastructure is then able to set up and evaluate all nested commutator expressions of the defined amplitudes with the Hamiltonian in a BCH expansion. This represents the conventional CCSD expressions,

$$\langle \Phi_i^a | e^{-(\hat{T}_1 + \hat{T}_2)} \hat{H} e^{(\hat{T}_1 + \hat{T}_2)} | 0 \rangle = | 0 \rangle, \quad (4)$$

$$\langle \Phi_{ij}^{ab} | e^{-(\hat{T}_1 + \hat{T}_2)} \hat{H} e^{(\hat{T}_1 + \hat{T}_2)} | 0 \rangle = | 0 \rangle. \quad (5)$$

The corresponding expression of all triples amplitudes is shown in Scheme 3. This will, in addition to the terms in

```
$order_E 2
$order_residuals 4
$class IA Tia(i,a) 1.0 E(a,i)
$class IJAB Tijab(ab,ij) 0.25 E(a,i)E(b,j); 1.0 E(a,i)E(b,j)
```

Scheme 2 Input required to generate the UHF CCSD equations.

eqn (4) and (5) include the triples equation and contributions to the singles and doubles amplitudes as:

$$\langle \Phi_i^a | e^{-(\hat{T}_1 + \hat{T}_2 + \hat{T}_3)} \hat{H} e^{(\hat{T}_1 + \hat{T}_2 + \hat{T}_3)} | 0 \rangle = 0, \quad (6)$$

$$\langle \Phi_{ij}^{ab} | e^{-(\hat{T}_1 + \hat{T}_2 + \hat{T}_3)} \hat{H} e^{(\hat{T}_1 + \hat{T}_2 + \hat{T}_3)} | 0 \rangle = 0, \quad (7)$$

$$\langle \Phi_{ijk}^{abc} | e^{-(\hat{T}_1 + \hat{T}_2 + \hat{T}_3)} \hat{H} e^{(\hat{T}_1 + \hat{T}_2 + \hat{T}_3)} | 0 \rangle = 0. \quad (8)$$

The CCSDT-1 (more specifically CCSDT-1a) equations are characterized by an approximate triples treatment for which, in addition to the CCSD equations, two terms are included in the triples equations, and one term is included which couples the T_3 amplitudes to the singles and one term which couples T_3 to the double amplitudes.

As any commutator, these can be added separately in a term-by-term manner as outlined in Schemes 3–6 (see the ESI†), this time, invoking our equation generation tool directly to generate each term.

$$t_i^a \leftarrow \langle \Phi_i^a | [\hat{H}, \hat{T}_3] | 0 \rangle. \quad (9)$$

$$t_{ij}^{ab} \leftarrow \langle \Phi_{ij}^{ab} | [\hat{H}, \hat{T}_3] | 0 \rangle. \quad (10)$$

$$t_{ijk}^{abc} \leftarrow \langle \Phi_{ijk}^{abc} | [\hat{F}, \hat{T}_3] + [\hat{H}, \hat{T}_2] | 0 \rangle. \quad (11)$$

Note that, in contrast to the MRCC generator tool by Kállay and Surján,³² ORCA-AGE is not able to generate arbitrary-order CC code, as the solver requires hand-coded infrastructure to perform a DIIS procedure including all amplitudes in the residual. For this purpose, internal data structures for tensors of rank 6 and 8 had to be explicitly defined, so that methods up to CCSDTQ are supported.

This way, ORCA-AGE II has been used to extend the ORCA functionality by CCSDT-1,2,3,4 and CCSDT as well as CC2 and CC3 UHF energies. The implementations have been verified against CFOUR⁹¹ and MRCC.

In order to test the limits of these implementations and the performance, calculations were carried out on small alkene chains and compared to CFOUR. As can be seen in Table 2, our implementation shows turnaround times that are in the ballpark of the CFOUR implementation, which is hand-coded and known to be efficient. Further analysis of the computational bottlenecks is underway and is expected to lead to further efficiency gains in the generated code.

Initially, our triples implementation has been restricted to spin-orbitals and UHF references. However, spin-orbital based wavefunctions, such as UHF-CCSDT, suffer from spin contamination, even with pure spin-references (such as ROHF references). Much research has already gone into eliminating spin contamination by spin adaptation, both for single and multi-reference methods.^{93–96} Since the resulting theory contains extra complexity, it is a prime candidate for code generation. Our work on spin-adapted triple excitation containing theories will be reported in due course.

```

$order_E 2
$order_residuals 4
$class IA Tia(i,a) 1.0 E(a,i)
$class IJAB Tijab(ab,ij) 0.25 E(a,i)E(b,j); 1.0 E(a,i)E(b,j)
$class IJKABC Tijkabc(abc,ijk) 1/36 E(a,i)E(b,j)E(c,k); 1.0 E(a,i)E(b,j)E(c,k)

```

Scheme 3 Input required to generate the UHF CCSDT equations.

Table 2 Average Sigma iteration time using UHF CCSDT. All electrons were correlated and a cc-pVTZ basis set was used.⁹² Calculations were performed on an AMD EPYC 75F3 with 200 GB of RAM reserved

Alkene	<i>n</i> _{basis}	Program	<i>t</i> _{iteration} (h)
Ethene	116	ORCA	1.2
		CFOUR	0.95
Propene	174	ORCA	37.3
		CFOUR	16.8

Generation of analytic gradients

A plethora of useful molecular properties can be calculated as energy derivatives with respect to a certain perturbation, such as nuclear gradients, harmonic vibrational frequencies or nuclear magnetic shielding.^{97,98} While these derivatives can be computed straightforwardly using numerical finite difference methods, it is also quite costly. Calculating the first derivative numerically requires a minimum of two energy calculations along the perturbation, with more calculations needed for increased accuracy. This quickly makes numerical gradient calculations unfeasible for larger molecules. More importantly, perhaps, is the fact that (especially higher-order) numeric derivatives tend to become unstable. Therefore, being able to evaluate analytic gradients is of vital importance, as their cost should not exceed that of approximately a single energy calculation.⁹⁹

Especially relevant for computing properties accurately is obtaining accurate geometries, which can be obtained through geometry optimizations. This involves minimizing the nuclear gradient, the energy derivative with respect to the nuclear coordinates. Due to geometry optimizations being a routine procedure in computational chemistry, nuclear gradients are a logical target to apply code generation to.

Since one of the cornerstones of code generation and ORCA-AGE II is generality, the aim was to build a general framework that would support arbitrary-order CI and CC nuclear gradients (and other derivatives). The starting point for gradients of non-variational methods is to formulate a Lagrangian (CI is taken as an example),^{100–105}

$$\mathcal{L}_{CI}(\boldsymbol{\kappa}, \mathbf{C}, \mathbf{z}) = \frac{\langle \Psi | \hat{H} | \Psi \rangle}{\langle \Psi | \Psi \rangle} + \sum_{p > q} z_{pq} f_{pq} \quad (12)$$

which needs to be made stationary with respect to all parameters. The key point for code generation is to formulate the stationary conditions and Lagrangian in contributions that are expressed as projected equations or expectation values containing second-quantized operators and that can be generalized to

arbitrary order. An example is this formulation of the unrelaxed 1-body density matrix,

$$\gamma_{pq} = \langle \Psi | E_q^p | \Psi \rangle. \quad (13)$$

With this restriction in mind, the gradient components that have to be generated are the equations to determine the CI coefficients/CC amplitudes and the unrelaxed density matrices. Equation solvers, such as for the amplitude equations, will have to be implemented by hand, as the AGE is not (yet) able to incorporate them in the generated modules. This is also the case for the so-called *Z*-vector equation, of which the solving provides the orbital relaxation contribution, z_{pq} .¹⁰⁴ By reformulating the CI energy functional in terms of the unrelaxed 1-body reduced density matrix (1RDM), γ and the 2-body reduced density matrix (2RDM), Γ ,

$$\mathcal{L}_{CI} = \sum_{pq} h_{pq} \gamma_{pq} + \sum_{pqrs} (pq|rs) \Gamma_{qs}^{pr} + \sum_{p > q} z_{pq} f_{pq} \quad (14)$$

it becomes clear that the orbital relaxation parameter can then be folded into the unrelaxed density matrices to construct the relaxed density matrices, γ' and Γ' ,

$$\mathcal{L}_{CI} = \sum_{pq} h_{pq} [\gamma_{pq}]' + \sum_{pqrs} (pq|rs) [\Gamma_{qs}^{pr}]', \quad (15)$$

with,

$$[\gamma_{pq}]' = \begin{cases} \gamma_{pq} + z_{pq}, & p > q \\ \gamma_{pq}, & p \leq q \end{cases} \quad (16)$$

$$[\Gamma_{qs}^{pr}]' = \begin{cases} \Gamma_{qs}^{pr} + z_{pq} \delta_{rs} \delta_{ri} - z_{pq} \delta_{rq} \delta_{ri}, & p > q \\ \Gamma_{qs}^{pr}, & p \leq q. \end{cases} \quad (17)$$

To obtain the final nuclear gradient expression, the derivative is taken with respect to the nuclear coordinates, \mathbf{R} , while using the orthonormal molecular orbitals (OMO) approach to ensure that the overlap matrix, \mathbf{S} , is well defined at every geometry.¹⁰⁶ This leads to the final expression of

$$\begin{aligned} \mathcal{L}^{(R)} = & \sum_{pq} h_{pq}^{(R)} [\gamma_{pq}]' + \sum_{pqrs} (pq|rs)^{(R)} [\Gamma_{qs}^{pr}]' \\ & + \sum_{pq} S_{pq}^{(R)} W_{pq}, \end{aligned} \quad (18)$$

with \mathbf{W} being defined as

$$W_{pq} = - \sum_r [\gamma_{pr}]' h_{rq} - 2 \sum_{rst} (pt|rs) [\Gamma_{st}^{rq}]'. \quad (19)$$



The superscript “(R)” on the integrals indicates that the derivative with respect to R is taken in the AO basis. The densities are therefore also first transformed to the AO basis before being contracted with the integral derivatives. As can be seen from the expression of the nuclear gradient, as long as the gradient can be expressed in terms of density matrices, any kind of CI or CC nuclear gradient can be generated up to arbitrary order. Currently, the following nuclear gradients have been implemented: RHF/UHF CID, CISD, CEPA(0), CCD, CCSD, as well as UHF CISDT/CCSDT, all of which were verified against numerical gradients as well as Kállay and Surján’s MRCC program.³²

The major bottleneck of these nuclear gradients was the 2RDM due to the layout of the matrix containers involved in its computation. Many contractions incurred a heavy I/O penalty in addition to not being able to utilize BLAS. As described above, this is where matrix containers can usefully be resorted in $\mathcal{O}(N^4)$ so that the most efficient BLAS operations are performed and the I/O operations are minimized. Given that already CCSD computationally scales as $\mathcal{O}(N^6)$, resorting will not have a significant impact on the computational performance of CC and CI theories. More importantly, the cost of resorting will be heavily outweighed by the gain in performance from being able to use BLAS operations. This resorting algorithm also keeps track of other resorted containers, so that no duplicates are created and so that they can be reused in other contractions. As can be seen from Fig. 1, the speedup can easily exceed a factor of 10–20 for larger system sizes.

To determine the efficiency of ORCA’s generated gradients, they have been compared against the MRCC program’s, which is able to generate these gradients on-the-fly for arbitrary order CI/CC theories. This is in contrast with the AGE, which generates code for a specific order of CI/CC, which is compiled into binary form prior to computation. The performance of both gradients is rather similar for smaller systems (Fig. 2), but when more basis functions are present, ORCA runs up to 20 times faster. This is where the effect of the data resorting becomes apparent since (i) the time to resort becomes negligible and (ii) BLAS can generate significant returns on larger tensors due to specialized multiplication methods. The lower performance of the MRCC might be attributed to the in-core parts of the calculation. At most 8 GB of memory is used for RHF CCSD,

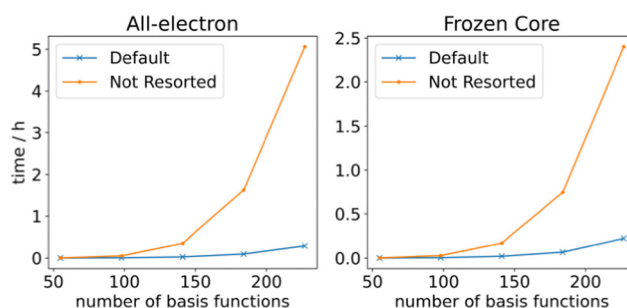


Fig. 1 RHF CCSD 2RDM performance with and without resorting matrix containers. The calculations were performed on linear alkanes of increasing length with a def2-TZVP basis set.

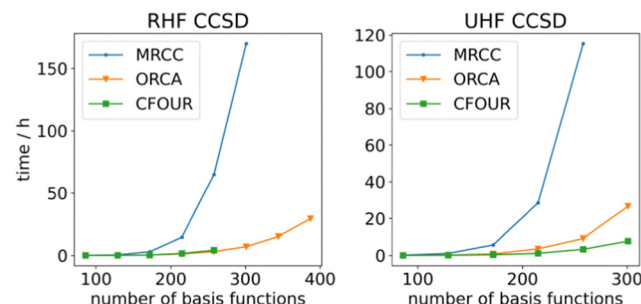


Fig. 2 Comparison of single RHF/UHF CCSD analytic gradient step between ORCA and MRCC on linear alkenes of increasing length in a def2-TZVP basis set. All electrons were correlated and the calculations were run in serial.

which is sub-optimal according to the MRCC output. Thus, the calculation becomes unfeasible for larger systems, whereas ORCA stores everything on disk and only loads the tensors into memory when needed. The UHF CCSD calculations were performed with 50 GB of memory. ORCA outperforms the MRCC gradients here as well despite MRCC not having to resort to out-of-core algorithms. This could be ascribed to the AGE’s ContractionEngine that is able to make optimal use of the available memory. A comparison has also been made against the hand-written CFOUR code.^{91,107} ORCA’s generated gradients perform approximately the same as CFOUR’s in the case of RHF CCSD. While larger calculations are certainly possible, we restricted the memory in CFOUR for consistency purposes such that CFOUR was not able to complete calculations with more than 258 basis functions. CFOUR does outperform ORCA by an approximate factor of 3 in the case of UHF CCSD. Overall, the generated code performs well, with it being able to handle system sizes of around 300–400 basis functions. Single gradient steps for these system sizes can be performed with a def2-TZVP¹⁰⁸ basis set within days on an AMD EPYC 75F3 CPU. These results indicate that code generation is a viable way to obtain reliable and performant code.

Internally contracted multireference coupled-cluster theory

Throughout quantum chemistry, we always strive for faster and more accurate theories to aid in our understanding of chemical systems. As mentioned before, CCSD(T) has been quite universally established as the “gold standard” in the single reference domain. In the multireference regime, however, no clear-cut “best” approach exists yet. Various approaches to transfer the coupled cluster Ansatz to multireference wave functions have been introduced,¹⁰⁹ some dating back to the late 1970s and early 80s.^{110–113} In our group, we focus on the internally contracted variant since it has several desirable properties, such as orbital invariance,¹¹⁴ a limited parameter space,⁶⁵ and size-extensivity.¹¹⁵ Furthermore, fic-MRCC theory is known to be significantly more accurate than fic-MRCI theory, even



when the BCH expansion of the similarity-transformed Hamiltonian is truncated at quadratic terms.¹¹⁶

Given a zeroth-order wave function $|0\rangle$ obtained from a run of a complete active space self-consistent field (CASSCF) calculation,

$$|0\rangle = \sum_I c_I |\Phi_I\rangle, \quad (20)$$

where $|\Phi_I\rangle$ are configuration state functions (CSFs), the Ansatz for the coupled cluster wave function can be written as

$$\begin{aligned} |\Psi = e^{\hat{T}}|0\rangle, \quad (21) \\ \hat{T} = & \frac{1}{2} t_{ab}^{ij} \hat{E}_i^a \hat{E}_j^b + t_{ai}^{ij} \hat{E}_i^a \hat{E}_j^i + \frac{1}{2} t_{iu}^{ij} \hat{E}_i^a \hat{E}_j^u \\ & + t_{ab}^{it} \hat{E}_i^a \hat{E}_t^b + t_{au}^{it} \hat{E}_i^a \hat{E}_t^u + t_{ua}^{it} \hat{E}_i^u \hat{E}_t^a \\ & + t_{uv}^{it} \hat{E}_i^u \hat{E}_t^v + \frac{1}{2} t_{ab}^{tu} \hat{E}_i^a \hat{E}_u^b + t_{av}^{tu} \hat{E}_i^a \hat{E}_u^v, \end{aligned} \quad (22)$$

with the cluster operator \hat{T} written in Einstein's summation convention for repeated indices. The energy and residuals are computed as in single-reference CC theory as the expectation value of the similarity-transformed Hamiltonian or by projecting the transformed Hamiltonian with functions from all excitation classes. To further simplify the theory, we also truncate the BCH expansion after quadratic terms.^{65,114} The resulting methodology is equivalent to scheme A from Hanauer and Köhn⁶⁵ omitting the reference relaxation. The outlined theory is not size extensive, but can become fully size-extensive with a minor modification.¹¹⁵ The latter is not considered in the present implementation.

This theory is very difficult to implement due to its large number of terms.⁶⁵ The working equations are derived with spatial orbitals using the elementary commutation rules of spin-traced excitation operators,³³

$$[\hat{E}_q^p, \hat{E}_s^i] = \hat{E}_s^i \delta_q^p - \hat{E}_q^p \delta_s^i. \quad (23)$$

The residual equations in their implicit form are provided in the supporting information. The presence of excitation operators involving active indices leads to a large number of non-vanishing equations.⁶⁵ In our formulation, fic-MRCC theory has 159 173 terms before removing contractions redundant by symmetry, and 49 186 terms after removal thereof. After factorization, the resulting 65 848 tensor contractions are translated to 3 765 810 lines of code. We remark that the number of equations is vastly different from the implementation of

Hanauer and Köhn, who report 5020 terms prior factorization for a CAS(6,6).⁶⁵ In the latter an additional truncation based on the number of active electrons limiting the rank of the reduced density matrix in the diagrammatic representation is employed, which can further reduce the number of equations, *e.g.* to 3523 terms for a CAS(2,2). The issue is presently under investigation.

A theory having so many terms places a high computational workload on the code generator, which was the primary reason for redeveloping the ORCA-AGE infrastructure. In particular, removing duplicate intermediates in the equation factorization step proved to be highly demanding, as that step creates 93 803 intermediates in the case of fic-MRCC theory, which are eventually pruned to 15 987 intermediates. In the previous version of ORCA-AGE, a simple algorithm for detecting duplicates was used that scaled as $\mathcal{O}(N^2)$, thus leading to impractically long generation times of about one month. In the updated version, this algorithm uses a hash table-based data compression technique with expected linear time instead, reducing the time to about 4 hours for the entire toolchain. In both cases, the toolchain, which has time-limiting steps parallelized with OpenMP threads, was run on 16 cores/32 threads.

If we now look at the generator from an end user's perspective, generating the code is also much simpler. All that is required is to define the excitation classes from eqn (22) in a user-friendly input file, an example of which is given in Scheme 4. Each line corresponds to an excitation class with an identifier, the amplitudes, and the excitation operators for that class. Optionally, contravariant projection operators⁹⁰ can be defined such that the projection functions are orthogonal to the excitation space. The generator itself features code that can create all necessary terms from the definition of the excitation classes, be it the similarity-transformed Hamiltonian through application of the BCH expansion, residuals through projection or the energy equations. Hence, everything from changing the cluster operator to the size of the BCH expansion is simple to program and quick to extend to other methods as well.

To exemplify the efficiency of the generated code, we consider two limiting cases in fic-MRCC theory: first, large systems with small active spaces, and second, systems with large active spaces. We further note that the contractions given below are asymptotically limiting, *i.e.*, they need not be the most expensive contractions for small systems. Large systems with small active spaces, *e.g.*, using triple- ζ basis sets and a CAS(2,2), are dominated by the 4-external term, which also appears in single-

```
$class IJAB Cijab(ab,ij) 0.5 E(a,i)E(b,j); 1/6 (2 E(a,i)E(b,j) + E(b,i)E(a,j))
$class IJTA Cijta(ta,ij) E(t,i)E(a,j); 1/3 (2 E(t,i)E(a,j) + E(a,i)E(t,j))
$class IJTU Cijtu(tu,ij) 0.5 E(t,i)E(u,j); E(t,i)E(u,j)
$class ITAB Citab(ab,it) E(a,i)E(b,t); 1/3 (2 E(a,i)E(b,t) + E(b,i)E(a,t))
$class ITAU Citau(at,iu) E(a,i)E(t,u)
$class ITUA Citua(ta,iu) E(t,i)E(a,u)
$class ITUV Cituv(ut,iv) E(u,i)E(t,v)
$class TUAB Ctuab(ab,tu) 0.5 E(a,t)E(b,u); E(a,t)E(b,u)
$class TUVA Ctuva(at,uv) E(a,u)E(t,v)
```

Scheme 4 Definition of the excitation classes for fic-MRCC theory (see also eqn (22)).



reference CC theory,

$$r_{ij}^{ab} = \sum_{cd} (ac|bd) t_{cd}^{ij}. \quad (24)$$

This term scales as $\mathcal{O}(n_{\text{inact}}^2 n_{\text{virt}}^4)$ and thus dominates the computational time for $n_{\text{virt}} \gg n_{\text{inact}}, n_{\text{act}}$. Therefore, it is crucial to fully optimize this term, which is complicated by the fact that the 4-external integrals must be stored on disk for their large size. This is where the hand-coded ContractionEngine functionality is employed: it minimizes I/O through reading large batches of the amplitudes and integrals (up to a given memory limit) and then applies a large-scale DGEMM operation to have maximum computational efficiency, consequently performing no worse than the best handwritten CC codes for this contraction.³⁴

The other extreme is given by systems with large active spaces. In these cases, the runtime is dominated by contractions such as

$$Y_{tuvwpa} \leftarrow \sum_{p_1 p_2 p_3 p_4 p_5} \gamma_{vtp_1 up_2}^{pwp_3 p_2 p_1} X_{p_1 p_2 p_3 p_4 p_5 a}, \quad (25)$$

which scales as $\mathcal{O}(n_{\text{act}}^{10} n_{\text{virt}})$ and consequently dominates the other contractions for $n_{\text{virt}} > n_{\text{inact}}, n_{\text{act}} \gtrsim 6$.

The tensor γ_5 is difficult for the CPU to manage because of its complicated structure with ten dimensions as well as its size (e.g., 8.59 GB for $n_{\text{act}} = 8$), thus leading to frequent cache misses if implemented naively with eleven nested loops. Such contractions are ideal candidates for the TTGT engine discussed above, as BLAS libraries carefully optimize both algorithms and cache usage. In this case, the generated code is reproduced in Scheme 5.

The TTGT engine first reorders the five-body density DC5 to optimally align and group the indices together, thus enabling a single large-scale DGEMM instruction to digest the contraction. As a result, explicit loops are only used to reorder the tensors, while the actual contraction is done with implicit loops in the DGEMM matrix-matrix multiplication. Compared to the same contraction implemented with plain for-loops, the TTGT scheme easily leads to a speedup by a factor >100 . All tensors are kept in memory since the space requirements are not as high as for the 4-external term and the number of active indices

is limited. The TTGT engine is also capable of accounting for indices associated with I/O and will dynamically adapt to load (sub-)tensors from disk in an optimal fashion and perform a DGEMM over the remaining non-I/O indices, if required.

The improvements made to the code generator in ORCA-AGE II now allow quite large systems to be computed with the fic-MRCC implementation. It should be noted that our generated code does not yet take advantage of point group symmetry and hence all calculations are performed under *C*1 symmetry. The implementation of point group symmetry is a logical next step that we are currently pursuing.

We will now present two calculations of tetradecene, C₁₄H₂₈, and naphthalene, C₁₀H₈, for which the requirements are close to the limits of computational resources for large systems with small active spaces and systems with large active spaces, respectively. Both systems were run in serial on an AMD EPYC™ 75F3 processor and use the def2-SVP basis set.¹⁰⁸ The tetradecene system uses a small CAS(2,2) active space. Thus, its 112 electrons are filled into 14 frozen core, 41 inactive, 2 active, and 279 virtual orbitals (336 in total). On average, a single iteration takes 6.58 hours. The calculation converges smoothly in 12 iterations for a total runtime of 3.3 days, a timeframe that is manageable for routine calculations. The naphthalene system, on the other hand, uses a CAS(10,10), and distributes 68 electrons among 10 frozen core, 19 inactive, 10 active, and 141 virtual orbitals (180 in total). Each iteration requires 11.35 hours to complete, and an additional 17.46 hours are spent computing the five-body density, which takes up 80.00 GB of memory. The total runtime for all 16 iterations is 8.3 days.

Finally, we present a series of calculations on linear polyene chains (see Fig. 3) at the fic-MRCI and fic-MRCC levels of theory, starting from ethene up until tetradecaheptaene, to systematically try to find the limits of the current implementation. The active space consists of the conjugated π -system and is thus increasing in size in tandem with the polyenes. We can conclude that a CAS(14,14) calculation, which in this case corresponds to a system size of 276 basis functions, is at the very limit of what is achievable with our fic-MRCI. A single-point calculation on tetradecaheptaene takes 3.5 days for 16 iterations. As can be seen, fic-MRCC is an order of magnitude

```

for (int t0 = 0; t0 < NActive; ++t0)
  for (int u0 = 0; u0 < NActive; ++u0)
    for (int v0 = 0; v0 < NActive; ++v0)
      for (int w0 = 0; w0 < NActive; ++w0)
        for (int p0 = 0; p0 < NActive; ++p0)
          for (int P1 = 0; P1 < NActive; ++P1)
            for (int P2 = 0; P2 < NActive; ++P2)
              for (int P3 = 0; P3 < NActive; ++P3)
                for (int P4 = 0; P4 < NActive; ++P4)
                  for (int P5 = 0; P5 < NActive; ++P5)
                    DC5_T({t0,u0,v0,w0,p0,P1,P2,P3,P4,P5}) = DC5({p0,v0,w0,t0,P3,P1,P2,u0,P4,P5});

BLAS_Add_Mat_x_Mat(false, false, NActive^5, NVirtual, NActive^5, 1.0, &DC5_T({0,0,0,0,0,0,0,0,0,0}), NActive^5, X({0,0,0,0,0,0}), NVirtual, 1.0, Y({0,0,0,0,0,0}), NVirtual);

```

Scheme 5 Generated code for the time-limiting step of fic-MRCC theory involving a five-body density γ_5 . This is an example of a BLAS call generated by the TTGT engine, where γ_5 is first aligned to the other tensors to enable a BLAS call, and the final BLAS DGEMM operation directly operates on the tensors, interpreting them as matrices. All indices starting with "p" refer to active indices in this context.



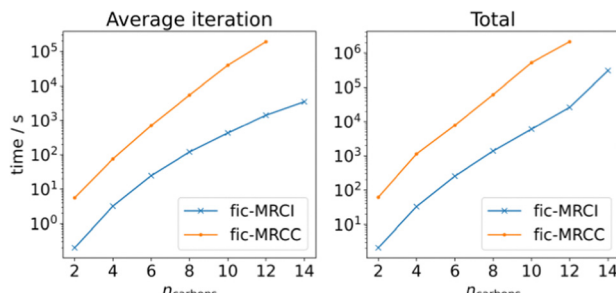


Fig. 3 Polyene calculations at fic-MRCI and fic-MRCC level, using a def2-SVP basis set, while increasing the number of carbons and simultaneously the active space, meaning $CAS(n_{\text{carbons}}, n_{\text{carbons}})$.

more expensive than fic-MRCI, meaning a $CAS(14,14)$ calculation could not be completed. The largest possible calculation was performed on dodecahexaene (238 basis functions) which took 24.5 days for 11 iterations.

From these examples, we see that increasing the size of the active space severely limits the system size to remain computationally feasible. This is both due to the asymptotic scaling, $\mathcal{O}(n_{\text{act}}^{10} n_{\text{virt}})$, as well as the difficulty of handling a large, high-dimensional tensor like γ_5 for the CPU, as discussed above. To this end, we are currently developing a version of fic-MRCC theory that only requires the four-body density.

In summary, ORCA-AGE II has been proven to be a performant toolchain that generates near-optimal code for the time-limiting steps of fic-MRCC theory. The code optimization strategies illustrated here are, of course, also applied to the non-limiting contractions in the code. However, despite the performant implementation, fic-MRCC theory remains a very time-intensive method due to the large number of contractions it contains.

Parallel code generation with MPI

Quantum chemistry methods, such as CC theory, have a cost that scales polynomially with respect to the number of basis

functions N , $\mathcal{O}(N^x)$. Hence, systems with many basis functions will take a long time to compute, unless further steps are taken. One way to approach this is to reduce the scaling of the methods through local approximation schemes, ideally ending at $x = 1$.⁴ However, even then computational demands grow with system size, to which the solution is to distribute the work among multiple processors, ideally dividing the work and thus the time perfectly among them. In this section, we will show how parallelization can be achieved in a fully automated way across any input theory that can be handled by ORCA-AGE II.

The most computationally demanding steps in electronic structure methods are typically the tensor contractions, so the parallelization effort should be focused on these. Considering that the parallelized code needs to be generated for an arbitrary number of contractions, a scheme is needed that would be efficient regardless of the number of contractions and would be able to handle the generality of the contractions. Hence, we opted for parallelization on per-contraction-basis, where the parallelization would occur only on the outermost loop. By additionally forcing the I/O to be restricted to the outermost loop (potentially by resorting matrix containers), it is ensured that no two processes will access the same target matrix simultaneously. A load-balancing scheme, in which one process works on a single expensive contraction while another process tackles multiple smaller contractions, is another route to solving this problem and is under active investigation.

An example of such parallelized code, based on eqn (26) can be found below in Scheme 6. In order to enforce the I/O of the target tensor to be restricted to the outermost loop, so-called pair or compound indices are used, which map a tuple of indices to a linear index and *vice versa*. In the case of eqn (26), the indices i, j are mapped to the pair index ij . Doing so also allows easy parallelization over restricted index lists, such as $i > j$. With the use of these compound indices, the contraction code for parallelized tensor contraction looks exactly like for a serial program. Tensors are loaded from disk, after which the contraction is evaluated (using BLAS) and the result is then stored on disk. The only extension that is needed

```

int pairIJAB_index_start, pairIJAB_index_stop;
PAL_DivideLoop(0, pairIJ[AUTOCL_IJAB].GetRows(), "<", pairIJAB_index_start, pairIJAB_index_stop);

for (int pairIJAB_index = pairIJAB_index_start; pairIJAB_index < pairIJAB_index_stop; ++pairIJAB_index) {
    const int i0=pairIJ[AUTOCL_IJAB](pairIJAB_index,0);
    const int j0=pairIJ[AUTOCL_IJAB](pairIJAB_index,1);

    load target matrix from disk

    for (int I1 = FirstInternal; I1 <= LastInternal; ++I1) {

        load source matrices from disk
        perform BLAS operation

    }

    store result on disk
}

```

Scheme 6 Semi-pseudo generated code of eqn (26) that has been parallelized over indices i, j using compound indices and ORCA parallel infrastructure.



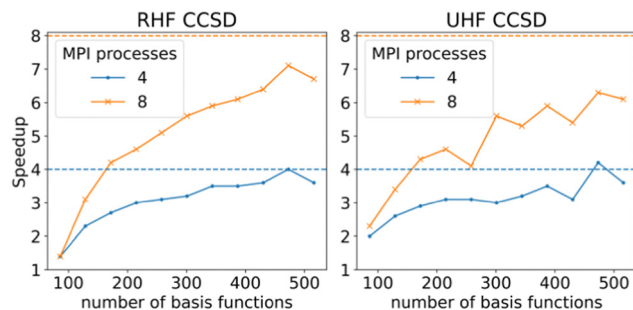


Fig. 4 Speed-up of CCSD Sigma equations by 4 and 8 processes as calculated for linear alkenes, ethene – dodecene in a def2-TZVP basis. The dashed lines indicate the ideal speedup. Calculations were performed on an AMD EPYC 75F3 processor.

is to distribute the list of compound indices to the processes in unique evenly sized batches, as defined by the `pairIJAB_index_start` and `pairIJAB_index_stop` variables.

$$\sigma_{ij}^{ab} \leftarrow \sum_{kc} (kj|bc)c_{ki}^{ca} \quad (26)$$

In order to check the performance of the parallelized code, benchmarks using the RHF- and UHF-CCSD methods were performed on a series of linear alkenes, from ethene to dodecene using the def2-TZVP basis set. Fig. 4 shows that the scaling for 4 processes is close to the ideal value when larger systems are treated. The situation is less ideal in the case of 8 processes, with the speed-up stagnating around 7 and 6 times for RHF- and UHF-CCSD, respectively. This is due to a small number of contractions incurring I/O penalties from forcing the target tensor to be accessed first.

A possible solution would be to gather the problematic contraction patterns and incorporate those in the Contraction-Engine as well to ensure maximum efficiency. Regardless, the initial parallel implementation performs well, especially considering that all of the code is generated entirely automatically with no custom intervention.

Perspective: automated code generation in quantum chemistry

In this section, we wish to address a few of the aspects which, in our opinion, are of central importance for the future of correlated wavefunction theory and where automatic code generation offers unique opportunities. These considerations are only partially of a genuine scientific nature, but we feel that it is useful to spell them out in the present context as they have far-reaching consequences for the way that implementation projects might be handled in the immediate future.

The art and science of writing computer programs that implement correlated wavefunction calculations began in the late 1960s and early 1970s. Ingenious programs were written by the best scientists in the field that took advantage of the state-of-the-art hardware at the time.^{117–121} Unfortunately, these

programs became obsolete with the next or second next generation of hardware. Since writing a correlated wavefunction code is an extremely technical and time-consuming undertaking, the codes have never been rewritten and the science and the effort that went into it are partially lost. Today, we are facing the very same problem of legacy codes that are no longer optimally adapted to modern computer facilities such as highly parallel supercomputers. At the same time, in an academic environment the novelty of writing another (e.g.) coupled cluster code, is necessarily limited since it has been done so many times in the past. Yet, it is still a difficult and time-consuming task. Consequently, finding the financial and human resources to tackle long and complicated re-implementation projects of known quantum chemical theories will become more and more difficult. It is precisely this aspect that we regard as one of the most important missions of automatic code generation: to ensure that theories can be implemented in an ever-shifting hardware landscape without investing years of programmer time. This is a problem that automatic code generation, in principle, is able to solve. However, in order to ensure that up-to-date code can indeed be generated one must simultaneously tackle the problem of “deep-integration”.

In order to explain the concept of “deep integration”, consider the commonly met situation, in which a code generator has been written by a very talented co-worker inside an academic research group who has since moved on and may no longer be available to ask questions, fix bugs or add new features. Furthermore, if the code generator was written in an unstable language, it may not even be executable anymore in its original form. There may be some code inside a given program package that was generated using these tools. If it was not meticulously documented how exactly that code was generated with which exact input using a given well-documented state of the generation chain, it will be impossible to re-generate that code. If the generated code is facing some limitations (for example not being parallelized or not taking proper advantage of molecular symmetry) the whole project will start from scratch when the need arises to implement such features.

In order to avoid such unproductive cycles, it will therefore be necessary to more tightly integrate the code generator itself as well as the generated code with the host program. This does not preclude the possibility that a given code generator can generate code for different host programs. The ideal situation that we envision, and to a large extent have realized in the present incarnation of ORCA-AGE II, is that the developer only submits their Ansatz in the form of an input file and expressed in the language of second quantization into the source code repository. Everything else from this point must proceed automatically: generation and factorization of equations, generation of host specific high-level code and insertion of this code in the host program. In this way, it can be ensured that all generated code is of uniform quality and reflects the latest state of development of the code generation chain. It will also ensure that the origin of all generated code is unambiguous and hence, well documented and reproducible. Obviously, for this concept to work, the source code of the code generator itself



must also be part of the source code repository. A master build then proceeds by first generating the code generation chain which subsequently triggers the generation of actual code as described above. To this end, ORCA has a module ORCA-AUTOCLI, that essentially consists of a framework of solvers and task organizers that trigger the various generated codes to generate Sigma-vectors, energy expressions, gradients *etc.* No generated code is inserted elsewhere in the program.

We believe, that following this strategy, the curse of legacy code can be overcome and the generated code can be optimally adapted to different hardware. In fact, if new hardware emerges, the only thing that needs to change is the final step of the generation that translates factorized equations into high-level code. For a new hardware, a new module must be added to the code generation chain that produces hardware specific code. Alternatively, the new module could make use of emerging libraries such as Kokkos¹²² or HPX.¹²³ This becomes an attractive possibility since no human time is involved in redoing quantum chemical code. Such a strategy would also allow for an optimal collaboration between quantum chemists and computer scientists since the chemistry and computer sciences tasks are cleanly separated from each other.

While we believe that solving the legacy code problem might be the most important mission for automatic code generation, there are other, more obvious advantages:

1. The generation of code implementing complex methods can proceed in a matter of hours instead of years.
2. Theories like fic-MRCC that are far too complex for humans, can be readily implemented in a reliable and efficient manner. This become more and more important since the readily implementable correlation methods tend to have been implemented already many times.
3. Once the toolchain is properly debugged, the generated code will be highly reliable and will produce correct results. This will save humongous amounts of debugging time that any human written code will have to go through.

Effectively, we envision a clearer partitioning of quantum chemistry codes in the future into low-level, mid-level, and high-level parts, to be explicated below. While the exact boundaries between the hierarchy of codes will be somewhat fluid, we nonetheless believe that we identified the three main (future) development areas of quantum chemistry codes.

Under “low-level,” we understand the foundational code of any quantum chemical software package that provides basic quantities such as molecular integrals and other general-purpose libraries used throughout the codes, *e.g.*, a library for arbitrary-dimensional tensors. Integral libraries already exist (for example, Libint,¹²⁴ SHARK¹²⁵ and libcint,¹²⁶ to name but a few) and have been extensively tuned for shortest possible runtimes. Interestingly, specialized code generation has also been employed for the integral libraries Libint¹²⁴ and SHARK,^{77,127} as especially loop unrolling allows the compiler to generate the most efficient code. Other low-level libraries include BLAS, which allows peak efficiency for the ubiquitous matrix multiplications in modern-day quantum chemistry codes. As a side note, general BLAS-like libraries for arbitrary tensors that may become more

pervasive in the future would also fall in this category. Noteworthy examples are TBLIS¹²⁸ and GETT,⁴³ among others.^{44,46}

Under our classification, the mid-level code would mainly comprise common algorithms that are implemented by hand, such as general solvers and drivers. Given a flexible interface, these common algorithms enable the (iterative) computation of the desired molecular properties without needing to copy-and-paste code, possibly with minor modifications depending on the actual method. Doing so guarantees that these core algorithms are free from errors since there is only the library that needs to be tested; and not multiple, slightly different implementations. Also, any improvements also apply across all implemented methods in a consistent fashion. In ORCA, we are steadily moving in this direction, starting with the Davidson and DIIS algorithms, and expect more changes by the time the next major version releases.

The highest level is reserved for the actual implementation of quantum chemical theories such as CCSD, CCSDT, fic-MRCC, and gradients. This is ideally enabled through a high-level interface that more closely resembles the mathematical equations or Ansätze rather than computer code. This can be achieved in many possible ways, each with its own benefits and drawbacks. In our group, we decided to focus on code generation since all contractions and tensors (with all their dimensions) are already known at compile time. Thus, there is no need to interpret the data on-the-fly, and the generated code can still be tailored to different architectures and different framework backends such as the ones mentioned in the introduction (CTF,^{44,45} libtensor,⁴⁶ LITF,⁴⁷ TCL,^{43,48} and TiledArray^{49,50}). Other approaches may include interpreters such as SIAL^{52,53,129,130} or direct usage of the aforementioned libraries. One might even generate code optimised for individual examples, given that the ideal factorisation depends on the size of the orbital subspaces. Eventually, only the mathematical equations would be stored in the code repository, which makes them easy to understand for new researchers as well as easy to validate and modify.

Our firm belief in these underlying trends has led us to significantly overhaul the entire architecture of ORCA, which has started with the code generator and the SHARK integral library^{77,127} for the fifth major version.¹²⁷ Further work has been done on the algorithms library, with more to come for the next major release. In this article, we outlined the latest developments in ORCA-AGE’s code generation capabilities, which showcases what we think will be representative of high-level interfaces in quantum chemical codes in the future.

Conclusions

In this article, we describe a newer version of ORCA-AGE, ORCA-AGE II, which is a complete overhaul of the previously introduced toolchain. Due to algorithmic improvements throughout the code (especially in the time-limiting steps) and a shift in programming language from PYTHON to C++, the toolchain is faster by a factor of ≈ 150 as measured while generating fic-MRCC theory. Its highly modular layout has also been refreshed,



enabling us to add new code engines such as the TTGT scheme easily. It is also simpler to use than the old toolchain as external dependencies were removed and because of an even tighter integration with the main ORCA source code: all computational modules can be regenerated with a simple command, which automatically brings new features and better code to existing modules as well.

The new toolchain has proven to be capable of generating even the most complicated theories, as demonstrated for fci-MRCC with its enormous number of terms generated through the commutation rules-based equation generator. We also showed that the toolchain is not tailored to specific problems, but rather general enough to allow a gradient framework for arbitrary theories to be developed with it. In both cases, the generated code is highly performant despite the large number of terms that must be computed. The AGE is even capable of producing well-performing parallelised code. Higher-order excitations, such as in CCSDT, can further be incorporated at minimal effort on the researcher's side.

In the end, developing automated code generators is beneficial for researchers as it allows them to spend their resources on their critical projects while at the same time transparently accounting for an efficient, production-level implementation. We believe that this is the direction in which *ab initio* quantum chemistry is evolving and will hence continue to align our development efforts on ORCA and ORCA-AGE with these trends.

Data availability

Original data from this work are provided as an open-access data set hosted by the Open Research Data Repository of the Max Planck Society at <https://doi.org/10.17617/3.CWGUUL>.

Conflicts of interest

There are no conflicts to declare.

Acknowledgements

The authors greatly appreciate clarifying comments by Ondřej Demel, Mihály Kállay, Andreas Köhn, Eric Neuscamman, Masaaki Saitow, Toru Shiozaki, and Alexander Y. Sokolov on the features of code generators in Table 1. The authors thankfully acknowledge funding by the Max Planck Society. M. H. L. further thanks the Fonds der Chemischen Industrie as well as the Studienstiftung des deutschen Volkes for support. Finally, we gratefully acknowledge funding of this work by the Deutsche Forschungsgemeinschaft (DFG, German Research Foundation) as part of the CRC 1639 NuMeriQS – project no. 511713970. Open Access funding provided by the Max Planck Society.

References

- 1 R. E. Watson, *Phys. Rev.*, 1960, **118**, 1036–1045.
- 2 R. E. Watson, *Phys. Rev.*, 1960, **119**, 1934–1939.
- 3 M. R. Silva-Junior, S. P. A. Sauer, M. Schreiber and W. Thiel, *Mol. Phys.*, 2010, **108**, 453–465.
- 4 C. Riplinger and F. Neese, *J. Chem. Phys.*, 2013, **138**, 034106.
- 5 C. Riplinger, P. Pinski, U. Becker, E. F. Valeev and F. Neese, *J. Chem. Phys.*, 2016, **144**, 024109.
- 6 R. R. Schaller, *IEEE Spectrosc.*, 1997, **34**, 52–59.
- 7 W. Meyer, in *Methods of Electronic Structure Theory*, ed. H. F. Schaefer III, Springer Science + Business Media, New York, 1977, vol. 3, pp. 413–446.
- 8 P. E. M. Siegbahn, *Int. J. Quantum Chem.*, 1980, **18**, 1229–1242.
- 9 T. Yanai, Y. Kurashige, M. Saitow, J. Chalupský, R. Lindh and P.-Å. Malmqvist, *Mol. Phys.*, 2017, **115**, 2077–2085.
- 10 S. Hirata, *Theor. Chem. Acc.*, 2006, **116**, 2–17.
- 11 C. L. Janssen and H. F. Schaefer III, *Theor. Chim. Acta*, 1991, **79**, 1–42.
- 12 G. C. Wick, *Phys. Rev.*, 1950, **80**, 268–272.
- 13 I. Shavitt and R. J. Bartlett, *Many-Body Methods in Chemistry and Physics: MBPT and Coupled-Cluster Theory*, Cambridge University Press, Cambridge, 2009.
- 14 S. Hirata, *J. Phys. Chem. A*, 2003, **107**, 9887–9897.
- 15 A. A. Auer, G. Baumgartner, D. E. Bernholdt, A. Bibireata, V. Choppella, D. Cociorva, X. Gao, R. Harrison, S. Krishnamoorthy, S. Krishnan, C.-C. Lam, Q. Lu, M. Nooijen, R. Pitzer, J. Ramanujam, P. Sadayappan and A. Sibiryakov, *Mol. Phys.*, 2006, **104**, 211–228.
- 16 T. Shiozaki, M. Kamiya, S. Hirata and E. F. Valeev, *Phys. Chem. Chem. Phys.*, 2008, **10**, 3358.
- 17 M. K. MacLeod and T. Shiozaki, *J. Chem. Phys.*, 2015, **142**, 051103.
- 18 K. R. Shamasundar, G. Knizia and H.-J. Werner, *J. Chem. Phys.*, 2011, **135**, 054101.
- 19 E. Neuscamman, T. Yanai and G. K.-L. Chan, *J. Chem. Phys.*, 2009, **130**, 124102.
- 20 E. Neuscamman, T. Yanai and G. K.-L. Chan, *J. Chem. Phys.*, 2009, **130**, 169901.
- 21 M. Saitow, Y. Kurashige and T. Yanai, *J. Chem. Phys.*, 2013, **139**, 044118.
- 22 M. Saitow, Y. Kurashige and T. Yanai, *J. Chem. Theory Comput.*, 2015, **11**, 5120–5131.
- 23 M. Saitow and T. Yanai, *J. Chem. Phys.*, 2020, **152**, 114111.
- 24 M. Nooijen and V. Lotrich, *J. Mol. Struct.: THEOCHEM*, 2001, **547**, 253–267.
- 25 L. Kong, K. R. Shamasundar, O. Demel and M. Nooijen, *J. Chem. Phys.*, 2009, **130**, 114101.
- 26 L. Kong, PhD Thesis, University of Waterloo, 2009.
- 27 A. Köhn, G. W. Richings and D. P. Tew, *J. Chem. Phys.*, 2008, **129**, 201103.
- 28 A. Köhn, *J. Chem. Phys.*, 2009, **130**, 104104.
- 29 J. Paldus and H. C. Wong, *Comput. Phys. Commun.*, 1973, **6**, 1–7.
- 30 H. C. Wong and J. Paldus, *Comput. Phys. Commun.*, 1973, **6**, 9–16.
- 31 Z. Csépés and J. Pipek, *J. Comput. Phys.*, 1988, **77**, 1–17.
- 32 M. Kállay and P. R. Surján, *J. Chem. Phys.*, 2001, **115**, 2945–2954.



33 T. Helgaker, P. Jørgensen and J. Olsen, *Molecular Electronic-Structure Theory*, John Wiley & Sons, Ltd, Chichester, 2000.

34 M. Krupička, K. Sivalingam, L. Huntington, A. A. Auer and F. Neese, *J. Comput. Chem.*, 2017, **38**, 1853–1868.

35 A. Hartono, A. Sibiryakov, M. Nooijen, G. Baumgartner, D. E. Bernholdt, S. Hirata, C.-C. Lam, R. M. Pitzer, J. Ramanujam and P. Sadayappan, in *Computational Science – ICCS 2005*, ed. V. S. Sunderam, G. D. van Albada, P. M. A. Sloot and J. J. Dongarra, Springer Berlin Heidelberg, Berlin, Heidelberg, 2005, vol. 3514, pp. 155–164.

36 P.-W. Lai, H. Zhang, S. Rajbhandari, E. Valeev, K. Kowalski and P. Sadayappan, *Proc. Comput. Sci.*, 2012, **9**, 412–421.

37 A. D. Bochevarov and C. D. Sherrill, *J. Chem. Phys.*, 2004, **121**, 3374–3383.

38 A. Hartono, Q. Lu, X. Gao, S. Krishnamoorthy, M. Nooijen, G. Baumgartner, D. E. Bernholdt, V. Choppella, R. M. Pitzer, J. Ramanujam, A. Rountev and P. Sadayappan, in *Computational Science – ICCS 2006*, ed. V. N. Alexandrov, G. D. van Albada, P. M. A. Sloot and J. Dongarra, Springer Berlin Heidelberg, Berlin, Heidelberg, 2006, vol. 3991, pp. 267–275.

39 A. Engels-Putzka and M. Hanrath, *J. Chem. Phys.*, 2011, **134**, 124106.

40 J. F. Stanton, J. Gauss, J. D. Watts and R. J. Bartlett, *J. Chem. Phys.*, 1991, **94**, 4334–4345.

41 C. L. Lawson, R. J. Hanson, D. R. Kincaid and F. T. Krogh, *ACM Trans. Math. Software*, 1979, **5**, 308–323.

42 M. Hanrath and A. Engels-Putzka, *J. Chem. Phys.*, 2010, **133**, 064108.

43 P. Springer and P. Bientinesi, *ACM Trans. Math. Software*, 2018, **44**, 1–29.

44 E. Solomonik, D. Matthews, J. Hammond and J. Demmel, *2013 IEEE 27th International Symposium on Parallel and Distributed Processing*, 2013.

45 E. Solomonik, D. Matthews, J. R. Hammond, J. F. Stanton and J. Demmel, *J. Parallel Distrib. Comput.*, 2014, **74**, 3176–3190.

46 E. Epifanovsky, M. Wormit, T. Kuš, A. Landau, D. Zuev, K. Khistyayev, P. Manohar, I. Kaliman, A. Dreuw and A. I. Krylov, *J. Comput. Chem.*, 2013, **34**, 2293–2309.

47 D. Kats and F. R. Manby, *J. Chem. Phys.*, 2013, **138**, 144101.

48 P. Springer, Tensor Contraction Library (TCL), <https://github.com/springer13/tcl>, (accessed September 20, 2021).

49 J. A. Calvin and E. F. Valeev. TiledArray: A general-purpose scalable block-sparse tensor framework, <https://github.com/valeevgroup/tiledarray>, (accessed June, 30, 2021).

50 J. A. Calvin, C. A. Lewis and E. F. Valeev, *Proceedings of the 5th Workshop on Irregular Applications: Architectures and Algorithms*, 2015.

51 N. Jindal, *PhD Thesis*, University of Florida, 2015.

52 E. Deumens, V. F. Lotrich, A. Perera, M. J. Ponton, B. A. Sanders and R. J. Bartlett, *Wiley Interdiscip. Rev.: Comput. Mol. Sci.*, 2011, **1**, 895–901.

53 E. Deumens, V. F. Lotrich, A. S. Perera, R. J. Bartlett, N. Jindal and B. A. Sanders, *Annual Reports in Computational Chemistry*, Elsevier, 2011, vol. 7, pp. 179–191.

54 H.-J. Werner, P. J. Knowles, G. Knizia, F. R. Manby and M. Schütz, *Wiley Interdiscip. Rev.: Comput. Mol. Sci.*, 2012, **2**, 242–253.

55 J. M. Herbert and W. C. Ermler, *Comput. Chem.*, 1998, **22**, 169–184.

56 M. Kállay and P. R. Surján, *J. Chem. Phys.*, 2000, **113**, 1359–1365.

57 K. Kowalski, J. R. Hammond, W. A. de Jong, P.-D. Fan, M. Valiev, D. Wang and N. Govind, in *Computational Methods for Large Systems*, ed. J. R. Reimers, John Wiley & Sons, Inc., Hoboken, NJ, USA, 2011, pp. 167–200.

58 H. J. J. van Dam, W. A. de Jong, E. Bylaska, N. Govind, K. Kowalski, T. P. Straatsma and M. Valiev, *Wiley Interdiscip. Rev.: Comput. Mol. Sci.*, 2011, **1**, 888–894.

59 S. Hirata, *J. Chem. Phys.*, 2004, **121**, 51–59.

60 S. Hirata, P.-D. Fan, A. A. Auer, M. Nooijen and P. Piecuch, *J. Chem. Phys.*, 2004, **121**, 12197–12207.

61 T. Shiozaki, M. Kamiya, S. Hirata and E. F. Valeev, *J. Chem. Phys.*, 2008, **129**, 071101.

62 B. Vlaisavljevich and T. Shiozaki, *J. Chem. Theory Comput.*, 2016, **12**, 3781–3787.

63 K. Chatterjee and A. Y. Sokolov, *J. Chem. Theory Comput.*, 2019, **15**, 5908–5924.

64 I. M. Mazin and A. Y. Sokolov, *J. Chem. Theory Comput.*, 2021, **17**, 6152–6165.

65 M. Hanauer and A. Köhn, *J. Chem. Phys.*, 2011, **134**, 204111.

66 D. Datta, L. Kong and M. Nooijen, *J. Chem. Phys.*, 2011, **134**, 214116.

67 D. Datta and M. Nooijen, *J. Chem. Phys.*, 2012, **137**, 204107.

68 O. Demel, D. Datta and M. Nooijen, *J. Chem. Phys.*, 2013, **138**, 134108.

69 M. Nooijen, O. Demel, D. Datta, L. Kong, K. R. Shamasundar, V. Lotrich, L. M. Huntington and F. Neese, *J. Chem. Phys.*, 2014, **140**, 081102.

70 J. A. Black, A. Waigum, R. G. Adam, K. R. Shamasundar and A. Köhn, *J. Chem. Phys.*, 2023, **158**, 134801.

71 W. Kutzelnigg and D. Mukherjee, *J. Chem. Phys.*, 1997, **107**, 432–449.

72 F. A. Evangelista, *J. Chem. Phys.*, 2022, **157**, 064111.

73 K. Sivalingam, M. Krupička, A. A. Auer and F. Neese, *J. Chem. Phys.*, 2016, **145**, 054104.

74 L. M. J. Huntington, M. Krupička, F. Neese and R. Izsák, *J. Chem. Phys.*, 2017, **147**, 174104.

75 F. Neese, *Wiley Interdiscip. Rev.: Comput. Mol. Sci.*, 2012, **2**, 73–78.

76 F. Neese, *Wiley Interdiscip. Rev.: Comput. Mol. Sci.*, 2017, **8**, e1327.

77 F. Neese, F. Wennmohs, U. Becker and C. Riplinger, *J. Chem. Phys.*, 2020, **152**, 224108.

78 T. Shiozaki, *Wiley Interdiscip. Rev.: Comput. Mol. Sci.*, 2018, **8**(1), e1331.

79 K. Raghavachari, G. W. Trucks, J. A. Pople and M. Head-Gordon, *Chem. Phys. Lett.*, 1989, **157**, 479–483.

80 Y. J. Bomble, J. F. Stanton, M. Kállay and J. Gauss, *J. Chem. Phys.*, 2005, **123**, 054101.

81 S. A. Kucharski and R. J. Bartlett, *J. Chem. Phys.*, 1992, **97**, 4282–4288.



82 J. Gauss and J. F. Stanton, *J. Chem. Phys.*, 2002, **116**, 1773–1782.

83 Y. S. Lee and R. J. Bartlett, *J. Chem. Phys.*, 1984, **80**, 4371–4377.

84 Y. S. Lee, S. A. Kucharski and R. J. Bartlett, *J. Chem. Phys.*, 1984, **81**, 5906–5912.

85 Y. S. Lee, S. A. Kucharski and R. J. Bartlett, *J. Chem. Phys.*, 1985, **82**, 5761.

86 M. Urban, J. Noga, S. J. Cole and R. J. Bartlett, *J. Chem. Phys.*, 1985, **83**, 4041–4046.

87 J. Noga, R. J. Bartlett and M. Urban, *Chem. Phys. Lett.*, 1987, **134**, 126–132.

88 J. Gauss and J. F. Stanton, *Phys. Chem. Chem. Phys.*, 2000, **2**, 2047–2060.

89 Y. He, Z. He and D. Cremer, *Theor. Chem. Acc.*, 2001, **105**, 182–196.

90 P. Pulay, S. Saebo and W. Meyer, *J. Chem. Phys.*, 1984, **81**, 1901–1905.

91 D. A. Matthews, L. Cheng, M. E. Harding, F. Lipparini, S. Stopkowicz, T. C. Jagau, P. G. Szalay, J. Gauss and J. F. Stanton, *J. Chem. Phys.*, 2020, **152**, 214108.

92 T. H. Dunning, *J. Chem. Phys.*, 1989, **90**, 1007–1023.

93 B. G. Adams and J. Paldus, *Phys. Rev. A: At., Mol., Opt. Phys.*, 1979, **20**, 1–17.

94 N. Herrmann and M. Hanrath, *J. Chem. Phys.*, 2020, **153**, 164114.

95 D. A. Matthews, J. Gauss and J. F. Stanton, *J. Chem. Theory Comput.*, 2013, **9**, 2567–2572.

96 D. A. Matthews and J. F. Stanton, *J. Chem. Phys.*, 2015, **142**, 064108.

97 F. Jensen, *Introduction to Computational Chemistry*, John Wiley & Sons, 2017.

98 P. Jørgensen and J. Simons, *J. Chem. Phys.*, 1983, **79**, 334–357.

99 P. Pulay, in *Modern Electronic Structure Theory*, ed. D. R. Yarkony, World Scientific, Singapore, 1995, vol. 2, p. 1191.

100 E. Salter, G. W. Trucks and R. J. Bartlett, *J. Chem. Phys.*, 1989, **90**, 1752–1766.

101 J. Gauss, W. J. Lauderdale, J. F. Stanton, J. D. Watts and R. J. Bartlett, *Chem. Phys. Lett.*, 1991, **182**, 207–215.

102 K. Hald, A. Halkier, P. Jørgensen, S. Coriani, C. Hättig and T. Helgaker, *J. Chem. Phys.*, 2003, **118**, 2985–2998.

103 A. C. Scheiner, G. E. Scuseria, J. E. Rice, T. J. Lee and H. F. Schaefer III, *J. Chem. Phys.*, 1987, **87**, 5361–5373.

104 N. C. Handy and H. F. Schaefer III, *J. Chem. Phys.*, 1984, **81**, 5031–5033.

105 K. Kristensen, P. Jørgensen, A. J. Thorvaldsen and T. Helgaker, *J. Chem. Phys.*, 2008, **129**, 214103.

106 T. Helgaker and P. Jørgensen, in *Methods in Computational Molecular Physics*, ed. S. Wilson and G. H. F. Diercksen, Plenum, New York, 1992.

107 J. Gauss, J. F. Stanton and R. J. Bartlett, *J. Chem. Phys.*, 1991, **95**, 2623–2638.

108 F. Weigend and R. Ahlrichs, *Phys. Chem. Chem. Phys.*, 2005, **7**, 3297–3305.

109 D. I. Lyakh, M. Musiał, V. F. Lotrich and R. J. Bartlett, *Chem. Rev.*, 2012, **112**, 182–243.

110 I. Lindgren, *Int. J. Quantum Chem.*, 1978, **14**, 33–58.

111 B. Jeziorski and H. J. Monkhorst, *Phys. Rev. A: At., Mol., Opt. Phys.*, 1981, **24**, 1668–1681.

112 W. D. Laidig and R. J. Bartlett, *Chem. Phys. Lett.*, 1984, **104**, 424–430.

113 A. Banerjee and J. Simons, *Int. J. Quantum Chem.*, 1981, **19**, 207–216.

114 F. A. Evangelista and J. Gauss, *J. Chem. Phys.*, 2011, **134**, 114102.

115 M. Hanauer and A. Köhn, *J. Chem. Phys.*, 2012, **137**, 131103.

116 J. A. Black and A. Köhn, *J. Chem. Phys.*, 2019, **150**, 194107.

117 R. Ahlrichs, H. J. Böhm, C. Ehrhardt, P. Scharf, H. Schiffer, H. Lischka and M. Schindler, *J. Comput. Chem.*, 1984, **6**, 200–208.

118 H. Lischka, R. Shepard, F. B. Brown and I. Shavitt, *Int. J. Quantum Chem., Quantum Chem. Symp.*, 1981, **15**, 91–100.

119 J. Paldus, J. Čížek and I. Shavitt, *Phys. Rev. A: At., Mol., Opt. Phys.*, 1972, **5**, 50–67.

120 W. Meyer, *J. Chem. Phys.*, 1973, **58**, 1017–1035.

121 R. J. Bartlett and G. D. Purvis, *Int. J. Quantum Chem.*, 1978, **14**, 561–581.

122 C. R. Trott, D. Lebrun-Grandie, D. Arndt, J. Ciesko, V. Dang, N. Ellingwood, R. Gayatri, E. Harvey, D. S. Hollman, D. Ibanez, N. Liber, J. Madsen, J. Miles, D. Poliakoff, A. Powell, S. Rajamanickam, M. Simberg, D. Sunderland, B. Turcksin and J. Wilke, *IEEE Trans. Parallel Distrib. Syst.*, 2022, **33**, 805–817.

123 H. Kaiser, P. Diehl, A. Lemoine, B. Lelbach, P. Amini, A. Berge, J. Biddiscombe, S. Brandt, N. Gupta, T. Heller, K. Huck, Z. Khatami, A. Kheirkhahan, A. Reverdell, S. Shirzad, M. Simberg, B. Wagle, W. Wei and T. Zhang, *J. Open Source Software*, 2020, **5**, 2352.

124 E. F. Valeev and J. T. Fermann. Libint: A high-performance library for computing Gaussian integrals in quantum mechanics, <https://github.com/evaleev/libint>, (accessed September 16, 2021).

125 F. Neese, *J. Comput. Chem.*, 2023, **44**, 381–396.

126 Q. Sun, *J. Comput. Chem.*, 2015, **36**, 1664–1671.

127 F. Neese, *Wiley Interdiscip. Rev.: Comput. Mol. Sci.*, 2022, **12**, e1606.

128 D. A. Matthews, *arXiv*, 2017, preprint, arXiv:1607.00291, DOI: [10.48550/arxiv.1607.00291](https://doi.org/10.48550/arxiv.1607.00291).

129 V. Lotrich, N. Jindal, E. Deumens, R. J. Bartlett and B. A. Sanders, Final Report: The Super Instruction Architecture, 2013.

130 V. F. Lotrich, J. M. Ponton, A. S. Perera, E. Deumens, R. J. Bartlett and B. A. Sanders, *Mol. Phys.*, 2010, **108**, 3323–3330.

